Suppression of defect states in HfSiON gate dielectric films on *n*-type Ge(100) substrates

K. B. Chung, H. Seo, J. P. Long, and G. Lucovsky[a)]
Department of Physics, North Carolina State University, Raleigh, North Carolina 27695-8202, USA

(Received 2 August 2008; accepted 30 September 2008; published online 4 November 2008)

Defect states in HfO_2 and HfSiON films deposited on Ge(100) substrates were studied by spectroscopic ellipsometry (SE) and x-ray absorption spectroscopy (XAS). In addition, structural and compositional changes in these films were examined via medium energy ion scattering (MEIS). SE and XAS experiments revealed two distinct band edge defect states, located at 1.7 ± 0.1 eV and at 2.7 ± 0.1 below the conduction band edges of these films. The number of defect states in HfO_2 increased noticeably following postdeposition annealing (PDA), whereas in HfSiON, it showed only small increases following the same treatment. MEIS measurements showed that Ge diffusion into HfO_2 films was enhanced significantly by PDA as well; however, this effect was less pronounced in the HfSiON films. The suppression of defect state enhancement in HfSiON films was correlated with lower levels of Ge diffusion and increased structural stability with respect to HfO_2.
 [DOI: 10.1063/1.3005422]

As the aggressive scaling of Si-based complementary metal-oxide semiconductors (CMOS) approaches its fundamental physical limitations, various attempts to improve the device performance have been investigated by enhancing carrier mobility in the channel region and by modifying channel structure.[1,2] One possible modification of the channel region being considered at present involves replacing Si by alternative semiconductor substrate or channel materials, such as Ge, SiGe, or GaAs.[1,2] In particular, Ge has attracted considerable interest because it has a significantly higher intrinsic carrier mobility and a smaller band gap than Si does. These properties offer a number of advantages in a channel material, leading to improvements in the injection current density, the scaling of the supply voltage, shorter switching speeds, and lower power consumption.[3] Despite the excellent intrinsic properties of Ge, attempts to fabricate Ge-based devices have been hindered by the lack of a stable interface passivation oxide and an inherently lower thermal budget.

Other research groups have reported previously the application of high-κ gate oxides to Ge substrates.[1,2,4] They concluded that Ge substrates could be implemented in CMOS circuits for p-MOSFETs by introducing various interfacial layers, such as SiO_2, GeO_2, and Ge nitride, to prevent reactions between the high-κ gate oxide and the Ge substrate. However, these studies have reported that Ge devices have relatively high defect densities, of the order of $\sim 10^{12}$ cm^{-2}.[2,4] These defect states function as electrical traps both at the interface and in the film, leading to inferior device performance. In addition, none of these studies have assigned a specific origin to these defect states.

In this study, we have focused on the identification of defect states in HfO_2 and on a pseudoternary alloy of HfSiON, each deposited on Ge(100) substrates. For a qualitative comparison of defect states, the HfO_2 and HfSiON films were examined both by spectroscopic ellipsometry (SE) and by x-ray absorption spectroscopy (XAS). These experiments clearly indicate the presence of two specific types of conduction band edge defects in both high-κ oxides. They reveal that the number of defect states in HfO_2 increases significantly after a postdeposition annealing (PDA), although the number of defect states in similar HfSiON films increases significantly less. The structural and compositional changes in the depth direction of the HfO_2 and HfSiON films were depth profiled by medium energy ion scattering (MEIS). MEIS results indicate that Ge diffuses into both the as-deposited and the annealed HfO_2 films, whereas Ge diffusion is effectively blocked in the corresponding HfSiON films. Furthermore, MEIS spectra reveal that the HfO_2 film density changes due to crystallization following PDA. However, there is Hf–O bonding in the interfacial transition region between the Ge substrate and the HfSiON dielectric. Thus, changes in the defect states with the dielectric films, but not necessarily in the interfacial transition regions, are correlated with the incorporation of Ge into the films and with structural changes in the films.

A *n*-type Ge wafer was sequentially rinsed with de-ionized water, H_2O_2 (6%), methanol, NH_4OH (15%), and de-ionized water again, removing the native oxide layer and producing a flat Ge surface.[5] Immediately following this surface treatment, the Ge wafer was introduced into the vacuum load lock of a remote plasma-enhanced metal-organic chemical vapor deposition (RPE-MOCVD) chamber. A sacrificial, interfacial plasma-nitrided interfacial layer, and then a high-κ oxide film was then deposited by RPE-MOCVD, each at 300 °C. The sacrificial GeN_x layer had a thickness of 0.7 ± 0.1 nm and was grown in order to prevent direct reaction between the Ge substrate and the high-κ film, as well as substrate oxidation during the high-κ film deposition process. However, this interfacial GeN_x layer could possibly limit the attainable downscaling of equivalent oxide thickness because of a lower dielectric constant than the high-κ dielectrics. As an alternative approach unique to this study, the interfacial GeN_x layer was removed by using a 1 min PDA treatment in Ar at 800 °C, which was sufficient to dissociate Ge–N bonds in the interfacial layer.[6] Following the PDA and sacrificial layer removal, the high-κ films were assumed to be in direct contact with the Ge substrate. The

[a)]Author to whom correspondence should be addressed. Electronic addresses: lucovsky@ncsu.edu and gerry-lucovsky@ncsu.edu.

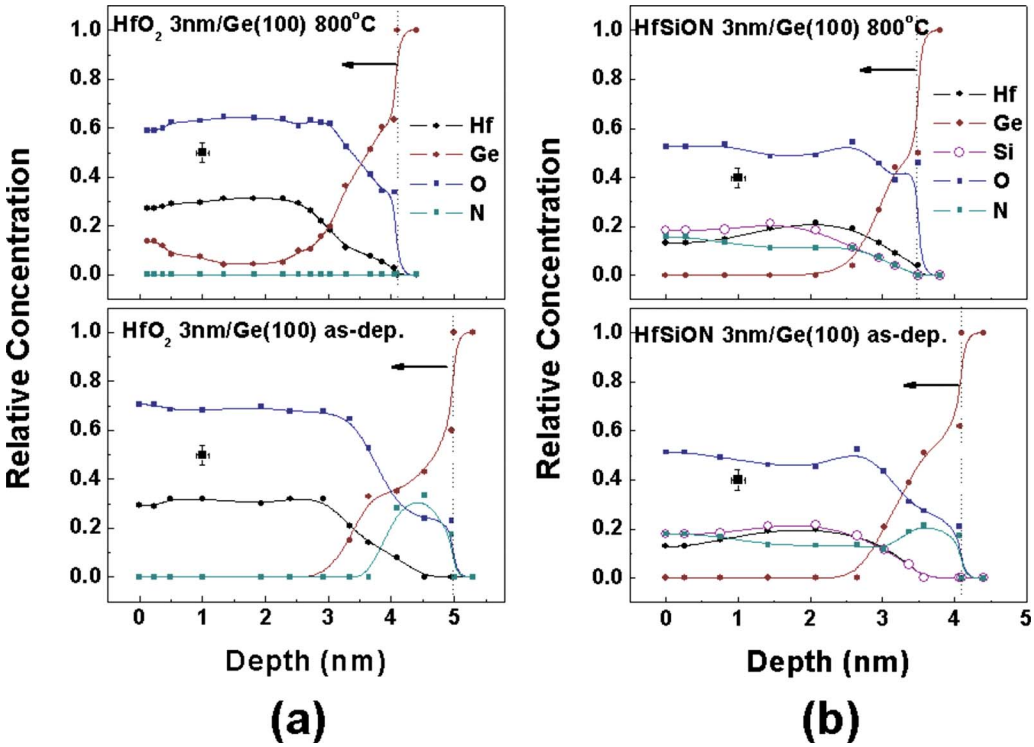

FIG. 1. (Color online) Compositional depth profile obtained by simulating MEIS energy spectra for as-deposited and annealed (a) HfO_2 films and (b) HfSiON films on Ge(100) substrates. Dotted line and arrow indicate the Ge substrates and the direction of the films. The spot with the error bar represents the fitting error in the depth direction and the relative concentration.

conduction band edge defect states of the high-κ film were then compared with the compositional changes in the film, both before and after PDA.

Figure 1 shows the compositional depth profile for HfO_2 and HfSiON films as a function of PDA temperature, obtained by MEIS, using H^+ ions with an incident energy of 100 keV. MEIS energy spectra were simulated by the KIDO program and used to generate compositional profiles.[8] An interfacial GeN_x layer, approximately 0.7–0.8 nm thick, is observed in the as-deposited films of both HfO_2 and HfSiON and is subsequently eliminated after PDA treatment. However, there is evidence that Hf–O bonds are formed at the Ge–Hf dielectric interface, indicating that the plasma nitride process did not effectively eliminate subcutaneous oxidation during dielectric film deposition. The width of the Hf peak in the HfO_2 films (not shown here) is slightly decreased after the PDA treatment, which means that the density of the HfO_2 films was increased as a result of nanograin changes that are evident in band edge *d*-state splittings.[7] Another interesting finding involves the behavior of Ge in the films after PDA treatment. The areal densities of Ge in the HfO_2 layer, which corresponded to the amount of Ge in the entire film, are 3.65×10^{15} and 6.04×10^{15} Ge atom/cm^2 for as-deposited (except an interfacial GeON layer) and annealed films, respectively. Similarly, the areal densities of Ge in the HfSiON films are 2.56×10^{15} and 3.35×10^{15} Ge atom/cm^2 for as-deposited and annealed films, respectively. HfO_2 films have a higher Ge concentration than both the as-deposited and the annealed HfSiON films. Moreover, the Ge concentration in the HfO_2 films is markedly increased after PDA, whereas the corresponding concentration of Ge in the HfSiON films is increased by a much smaller amount. This indicates that Ge diffusion is inhibited more effectively by HfSiON films. The relative ease with which Ge diffused into the HfO_2 films during annealing is attributed to by the removal of the interfacial GeN_x layer and the increased grain size in the HfO_2 films after the PDA treatments.

Imaginary dielectric function (ε_2) spectra for HfO_2 and HfSiON films on Ge(100) substrates are shown in Fig. 2. These spectra were extracted from a simple four-phase model, which was comprised of a Ge substrate, a GeON overlayer, a high-κ overlayer, and an ambient layer.[8] The best fit to this model was determined to be the one which minimized artifacts in the dielectric function below the conduction band edge caused by the strained Ge substrate. The

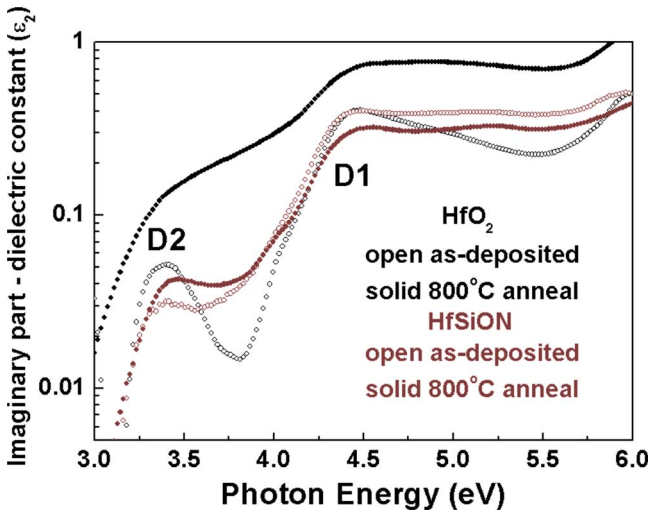

FIG. 2. (Color online) Imaginary dielectric function (ε_2) spectra from SE measurement for the as-deposited and annealed HfO_2 and HfSiON films on Ge(100) substrates.D_1 and D_2 indicate the defect states located below the conduction band edge.

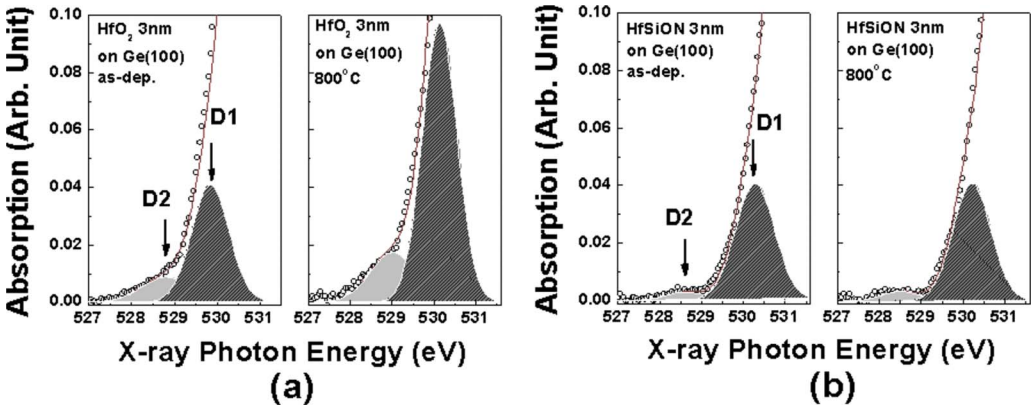

FIG. 3. (Color online) XAS spectra below the absorption edge of the O K_1 feature for (a) HfO_2 and (b) HfSiON films on Ge(100) substrates. Two deconvoluted peaks, labeled D_1 and D_2, indicate the defect states determined by Gaussian fitting of the XAS O K_1 edge spectra.

imaginary dielectric function spectra clearly depict two distinct types of energy states below the Hf $5d$ e_g conduction band edge states, which are located at approximately 6 eV.[9] D_1 and D_2 are designated as sub-band gap defect states because they are observed at 1.7 ± 0.1 and 2.7 ± 0.1 eV, respectively, below the conduction band edge states. Both defect states are observed in the as-deposited HfO_2 films and significantly increased after PDA. The defect states are both observed in the as-deposited HfSiON films as well; however, they show a much smaller increase after the PDAs. The D_2 state shows a small increase, but the D_1 state shows almost no change.

Figure 3 shows XAS O K_1 spectra over a narrow energy region below the Hf $5d$ e_g conduction band edge states for both HfO_2 and HfSiON films. In order to qualitatively analyze the defect states, the spectra also include Gaussian fits, which were performed in the detection limit of XAS, following background subtraction and peak normalization.[10] The Gaussian fits are composed of (i) band edge defect states below the Hf $5d$ e_g states, (ii) Hf $5d$ e_g states from which twofold degeneracy has been removed by a cooperative Jahn–Teller distortion, (iii) Hf $5d$ t_{2g} states for which threefold degeneracy has been removed similarly, and (iv) two features that correspond to Hf $6s$ and Hf $6p$ states.[11] However, the t_{2g} states of O K_1 edge in HfSiON films reflect the double band states caused by O p states hybridized with Si $3sp$ states in addition to Hf $5d$ t_{2g} states.[12] Consequently, the peak intensities of the Gaussian fits below Hf $5d$ e_g states in one sample could be compared those of the other samples in order to determine the relative quantities of the energy states. Figure 3 shows only the narrow energy region relevant to the defect features located below the conduction band edge. Like the ε_2 spectra, the Gaussian fits identify two different types of defect states, and they are located at similar energies below the Hf $5d$ e_g conduction band edge: 531.8 ± 0.2 eV. Relative changes in the intensities of the two defect states following the PDA are consistent with Ge diffusion and HfO_2 grain growth previously discussed with respect to the MEIS data. Based on these comparisons, the defect state (D_1) located ~530 eV is assigned to transitions that terminate in empty Hf^{3+} states in divacancy defects, clustered at grain boundaries.[9] The defect state (D_2) located at 528.7 eV is assigned to a divacancy defect that includes a Hf^{3+} divacancy and the incorporation of Ge into that defect arrangement as well. An increase in the number of HfO_2 defect states following PDA is clearly observed, ALthough similar effects in HfSiON are much smaller. Therefore, noncrystalline HfSiON films effectively suppress an increase in these divacancy defects, which is critical because such defects can function as sources for both fixed and oxide trapped charges.

In conclusion, the evolution of defect states was investigated in high-κ HfO_2 and HfSiON films deposited on Ge(100) substrates as a function of a PDA treatment. These high-κ films have two distinct types of band edge defect states located below their conduction band edges, which are related to the incorporation of Ge into the films, as well as to the structural evolution of the films. The number of defects present in the as-deposited HfO_2 films is higher than that in both the as-deposited and the annealed HfSiON films; furthermore, the number of defects in such HfO_2 films significantly increases through Ge diffusion and HfO_2 crystallization following PDA. These defects in HfSiON films are suppressed, which is due to Ge diffusion blocking and an enhanced structural stability over that of HfO_2.

This work was supported by the Korean Research Foundation Grant funded by the Korean Government (MOEHRD) (No. KRF-2007-357-C00020).

[1] G. Lucovsky, H. Seo, S. Lee, L. B. Fleming, M. D. Ulrich, J. Lüning, P. Lysaght, and G. Bersuker, Jpn. J. Appl. Phys., Part 1 **46**, 1899 (2007).
[2] C. O. Chui, F. Ito, and K. Saraswat, IEEE Trans. Electron Devices **53**, 1501 (2006).
[3] S. M. Sze, *Physics of Semiconductor Devices*, 2nd ed. (Wiley, New York, 1981).
[4] S. Takagi, T. Maeda, N. Taoka, M. Nishizawa, Y. Morita, K. Ikeda, Y. Yamashita, M. Nishikawa, H. Kumagai, R. Nakane, S. Sugahara, and N. Sugiyama, Microelectron. Eng. **84**, 2314 (2007).
[5] H. Seo, K. B. Chung, and G. Lucovsky (unpublished).
[6] K. Kutsuki, G. Okamoto, T. Hosoi, T. Shimura, and H. Watanabe, Appl. Phys. Express **47**, 2415 (2008).
[7] K. B. Chung, H. S. Chang, S. H. Lee, C. N. Whang, D.-H. Ko, H. Kim, D. W. Moon, and M.-H. Cho, Electrochem. Solid-State Lett. **8**, F51 (2005).
[8] D. E. Aspnes and A. A. Studna, Phys. Rev. B **27**, 985 (1983).
[9] G. Lucovsky, C. L. Hinkle, C. C. Fulton, N. A. Stoute, H. Seo, and J. Lüning, Radiat. Phys. Chem. **75**, 2097 (2006).
[10] J. Stöhr, *NEXAFS Spectroscopy* (Springer, New York, 1991).
[11] G. Lucovsky, C. C. Fulton, Y. Zhang, Y. Zou, J. Lüning, L. F. Edge, J. L. Whitten, R. J. Nemanich, H. Ade, D. G. Schlom, V. V. Afanase'v, A. Stesmans, S. Zollner, D. Triyoso, and B. R. Rogers, IEEE Trans. Device Mater. Reliab. **5**, 65 (2005).
[12] M.-H. Cho, K. B. Chung, C. N. Whang, D. W. Lee, and D.-H. Ko, Appl. Phys. Lett. **87**, 242906 (2005).